using the graphs presented in [11]. By using these graphs it can be shown that $S_{1,2}=2$ cm, $S_{2,3}=2.1$ cm, $S_{3,4}=2.18$ cm, $W_1=1.00$, $W_2=0.975$ cm, $W_3=1.00$ cm, $W_4=1.04$ cm, where $S_{r,r+1}$ and W_r are shown in Fig. 10.

The dimensions of the slits can be evaluated by using the formula (see [12])

$$Y_{r,r}=(d_r^2/3840)(\pi/b)^2\left(\operatorname{sech}\left(\frac{\pi}{2}\cdot\frac{W_r}{b}\right)\right)^{-2}\exp\left(-\frac{\pi}{b}\cdot\frac{\tau}{d_r}\right)$$

where K_e is a complete elliptic integral [13]. The above equation can solved numerically to obtain d_r. The input and the output sections can be designed by using tapered conductors and the lumped capacitors can be realized by shaping the tip of each bar.

References

[1] J. D. Rhodes and I. H. Zabalawi, "Design of selective linear phase filters with equiripple amplitude characteristics," *IEEE Trans. Circuits Syst.*, vol. CAS-25 pp. 989–1000, Dec. 1978.

[2] R. J. Wenxel, "Synthesis of combine and capacitively loaded interdigital band-pass filters of arbitrary bandwidth," *IEEE Trans. Microwave Theory Tech.*, vol. MTT-19, pp. 678–686, Aug. 1971.

[3] J. D. Rhodes, "A low-pass prototype network for microwave linear phase filters," *IEEE Trans. Microwave Theory Tech.*, vol. MTT-18, pp. 290–301, June 1970.

[4] J. H. Cloete, "Tables for nonminimum-phase even-degree low pass prototype networks for the design of microwave linear-phase filters," *IEEE Trans. Microwave Theory Tech.*, vol. MTT-27, pp. 123–128, Feb. 1979.

[5] J. D. Rhodes, "The generalized direct-coupled cavity linear phase filters," *IEEE Trans. Microwave Theory Tech.*, vol. MTT-13, pp. 308–313, June 1970.

[6] J. D. Rhodes, "The generalized interdigital linear phase filters," *IEEE Trans. Microwave Theory Tech.*, vol. MTT-18, pp. 301–307, June 1970.

[7] A. E. Williams and A. E. Atia, "Dual-mod canonical waveguide filters," *IEEE Trans. Microwave Theory Tech.*, vol. MTT-25, pp. 1021–1026, Dec. 1977.

[8] J. D. Rhodes, "The generalized interdigital networks," *IEEE Trans. Circuit Theory*, vol. CT-16, pp. 280–288, Aug. 1969.

[9] J. D. Rhodes, "Lecture notes on microwave circuit theory," Univ. Leeds, 1976.

[10] S. B. Chon, "Direct-coupled resonator filters," *Proc. IRE* vol. 45, pp. 187–196, Feb. 1957.

[11] W. J. Getsinger, "Coupled rectangular bars between parallel plates," *IEEE Trans. Microwave Theory Tech.* vol. MTT-10, pp. 65–72, Jan. 1962.

[12] J. K. Shimizu and E. M. T. Jones, "Coupled-transmissionline directional couplers," *IEEE Trans. Microwave Theory Tech.*, vol. MTT-6, pp. 402–410, Oct. 1958.

[13] M. Abramowitz and I. A. Stegun, Eds., *Handbook of Mathematical Functions with Formulas, Graphs, Mathematical Tables.* New York: Dover, 1964.

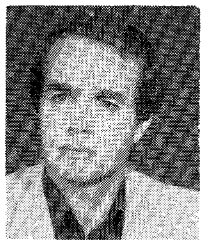

Isam Hasan Zabalawi (S'78–M'80) was born in Amman, Jordan, on October 29, 1950. He received the B.Sc. degree in electrical engineering from Cairo University, Egypt, and the M.Sc. and Ph.D degrees in electrical and electronic engineering from Leeds University, England, in 1974, 1976, and 1979, respectively. From 1974 to 1975 he was a System Engineer with Jordan Television.

Currently he is an Assistant Professor with the Department of Electrical Engineering, University of Jordan. His research interests are in the field of lumped and distributed circuits and systems.

Combining the Powers from Multiple-Device Oscillators

MOHAMMAD MADIHIAN, STUDENT MEMBER, IEEE, AND SHIZUO MIZUSHINA, MEMBER, IEEE

***Abstract*—This paper describes the results of power combining with multiple-device oscillators. A combiner circuit consisting of 3 oscillators and a directional coupler is analyzed. Conditions are set to obtain the maximum combining efficiency and a key approach is developed to control the frequency of the combiner. It is shown that the performance of the system is not seriously affected by the dissimilarity of the oscillators used in the combiner. A prototype 84-diode power combiner is constructed and total output power of 1.72 W with combining efficiency of 98.3 percent is obtained at 9.7 GHz. No fundamental limiting factor for the maximum number of devices to be combined was found.**

Manuscript received December 28, 1981; revised March 17, 1982.

The authors are with the Research Institute of Electronics, Shizuoka University, Hamamatsu 432, Japan.

I. Introduction

MICROWAVE POWER COMBINERS can be classified into two categories: 1) single circuit multiple-device structures, and 2) tree structures. In the former class, a number of devices contribute to the output power in a single circuit provided that the phase of the signal generated by each device is properly adjusted [1]–[3]. So

0018-9480/82/0800-1228$00.75 ©1982 IEEE

far, the maximum number of devices combined in a single cavity is 32 IMPATT's as reported by Hamilton [3]. In the latter class, the output powers from several single-device sources are summed to produce a higher output power at a single frequency [4]–[6]. Mizushina and coauthors [6] have combined 13 single-diode oscillators in tandem. Practically the number of devices in the former and the number of sources in the latter are limited because of the size and the circuit stability of the structures, respectively. So, one can incorporate both approaches to devise a class of combiners to increase the total number of devices; hence, the output power. Perhaps the reason for the void of any reported work on this subject has been the lack of an appropriate combining structure. For this purpose the combining circuit reported earlier by one of the authors [6] is useful. It combines the powers from 3 oscillators using a 3-dB short slot coupler [7] in conjunction with high-level injection-locking. The technique is fundamentally based on increasing the output power of a high-level injection-locked oscillator to the sum of the free running power and the injected power by properly adjusting the oscillator, and can be explained by oscillator injection-locking theory [8]–[10]. Using this circuit as a starting point to increase the number of devices that can be combined, we have succeeded in combining 84 Gunn diodes using one 12-diode plus two 36-diode oscillators. The output power obtained was 1.72 W, and the oscillation was quite stable. The present paper treats the operation of the combiner circuit by employing oscillator phase locking theory. It describes the conditions for optimum operation and demonstrates experimental results.

II. Circuit Operation of the Combiner

Fig. 1 represents the schematic diagram of the 3-oscillator power combining structure. Three oscillators and a matched load are connected to the four ports of a directional coupler. Under free running conditions oscillators 1, 2, and 3 generate maximum powers P_1, P_2, and P_3, respectively. Let the scattering matrix $[S]$ represent a lossless directional coupler with the coupling coefficients α and β [7]. Furthermore, let $a_k = |a_k| \exp(j\gamma_k)$ and $b_k = |b_k| \exp(j\lambda_k)$ be the power waves going into and out of kth port of the coupler, where $k = 1,2,3,4$, and γ_k, and λ_k are the phase of the power waves with respect to an appropriate reference plane. Using the scattering matrix $[S]$ the power waves b_k can be obtained in terms of a_k

$$\begin{bmatrix} b_1 \\ b_2 \\ b_3 \\ b_4 \end{bmatrix} = [S] \begin{bmatrix} a_1 \\ a_2 \\ a_3 \\ a_4 \end{bmatrix} = \begin{bmatrix} \alpha a_2 + j\beta a_3 \\ \alpha a_1 \\ j\beta a_1 \\ j\beta a_2 + \alpha a_3 \end{bmatrix} \tag{1}$$

where

$$[S] = \begin{bmatrix} 0 & \alpha & j\beta & 0 \\ \alpha & 0 & 0 & j\beta \\ j\beta & 0 & 0 & \alpha \\ 0 & j\beta & \alpha & 0 \end{bmatrix}$$

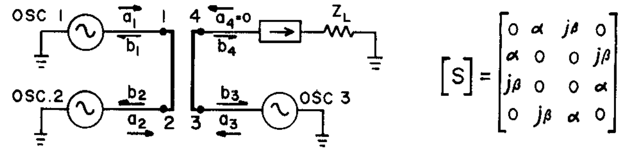

(a) (b)

Fig. 1. (a) Schematic diagram of the 3-oscillator power combiner. (b) Scattering matrix of the coupler in (a).

and

$$\alpha^2 + \beta^2 = 1.$$

The power wave a_1 from oscillator 1 is scattered into b_2 and b_3. b_2 is injected into oscillator 2. Oscillator 2 is then synchronized to oscillator 1 and the synchronized signal is indicated by a_2. Under proper conditions the output power of oscillator 2 can be as high as the sum of the free running power and the injected power [6]. This can be also verified by a nonlinear theory of synchronized oscillators using a van der Pol oscillator model [8], [9]. Applying the method of analysis described in [8] and [9] to the present circuit, one can write, after some manipulations, the set of following differential equations which govern the amplitude $|a_2|$ and the phase angle ϕ_{12} between a_1 and a_2:

$$\begin{aligned} (2Q_{ex2}/\omega_2|a_2|)\,d|a_2|/dt &= (3 - 3|a_2|^2/P_2 - |b_2|^2/P_2)(|b_2|/|a_2|)\cos\phi_{12} \\ &\quad - (2|b_2|^2/P_2)\cos^2\phi_{12} + (2\delta_2 Q_{ex2}|b_2|/|a_2|)\sin\phi_{12} \\ &\quad - |a_2|^2/P_2 - |b_2|^2/P_2 + 1 \end{aligned} \tag{2}$$

$$\begin{aligned} (2Q_{ex2}/\omega_2)\,d\gamma_2/dt &= (3 - |a_2|^2/P_2 - |b_2|^2/P_2)(|b_2|/|a_2|)\sin\phi_{12} \\ &\quad - (|b_2|^2/P_2)\sin 2\phi_{12} \\ &\quad - (2\delta_2 Q_{ex2}|b_2|/|a_2|)\cos\phi_{12} - 2\delta_2 Q_{ex2} \end{aligned} \tag{3}$$

where $\delta_2 = (\omega_1 - \omega_2)/\omega_2$ is the degree of detuning, ω_1 and ω_2 the angular frequency of oscillators 1 and 2, respectively, and Q_{ex2} is the external Q of oscillator 2. The steady-state solutions of $|a_2|$ and $\phi_{12} = \gamma_1 - \gamma_2$ can be obtained by setting $d|a_2|/dt = d\gamma_2/dt = 0$ in the above equations. As in [8], the synchronized signal power $|a_2|^2$ and the phase angle ϕ_{12} were calculated using a computer. The results are shown in Figs. 2 and 3 where $|a_2|^2$ and ϕ_{12} are plotted against the degree of detuning δ_2 for several $|b_2|^2/P_2$ over the synchronization range, assuming that oscillator 2 generates the maximum power P_2 under the free running condition. For every $|b_2|^2/P_2$ there exists an optimum δ_2 namely $\delta_{2op} = ((\omega_1 - \omega_2)/\omega_2)_{op}$, at which the power absorbed by oscillator 2 vanishes and $|a_2|^2$ becomes maximum

$$|a_2|^2_{max} = |a_2|^2|_{\delta_{2op}} = P_2 + |b_2|^2 = P_2 + \alpha^2|a_1|^2. \tag{4}$$

Similarly for oscillator 3 injected by b_3 the synchronized signal is a_3 and (2)–(4) hold by replacing subscripts 2 with 3, α with β, and by adding a $\pi/2$ term in the arguments for j in $j\beta$. The same applies to Figs. 2 and 3.

Equations (1)–(4) are sufficient to calculate the output power and the synchronization frequency of the combiner.

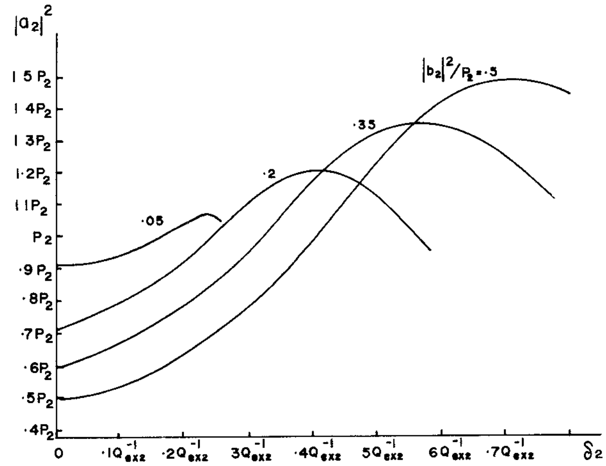

Fig. 2 The output power of synchronized oscillator 2 versus the degree of detuning for several synchronization power levels.

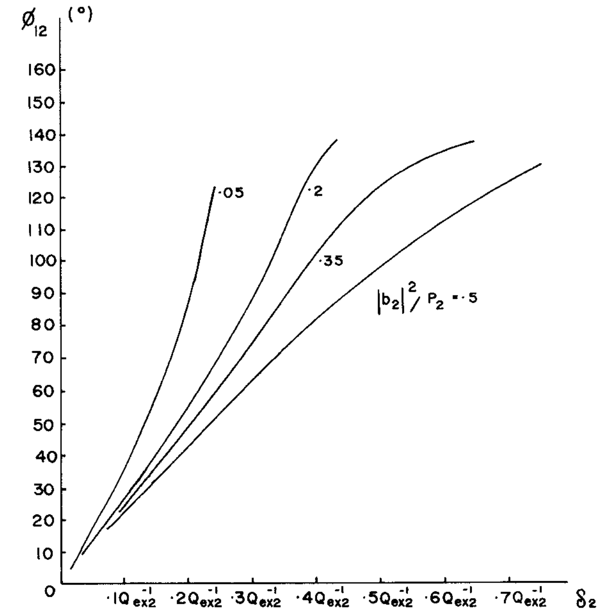

Fig. 3. The phase angle between oscillators 1 and 2 versus the degree of detuning for several synchronization power levels.

A. Output Power and Combining Efficiency

From (1) the output power P_c delivered to the matched load is given by

$$P_c = |b_4|^2 = \beta^2|a_2|^2 + \alpha^2|a_3|^2 + 2\alpha\beta|a_2|\cdot|a_3|\sin\phi_{32} \tag{5}$$

where ϕ_{32} is the phase angle between a_3 and a_2. Equation (5) takes its maximum when

$$\phi_{32} = \pi/2 \tag{6a}$$

$$|a_2|/|a_3| = \beta/\alpha. \tag{6b}$$

Physically (6) sets the conditions to have no power reflected back to oscillator 1, i.e., $b_1 = 0$. Substituting (6) into (5) the output power becomes

$$P_c = |a_2|^2 + |a_3|^2 \tag{7}$$

which may appear similar to the broken curve in Fig. 4

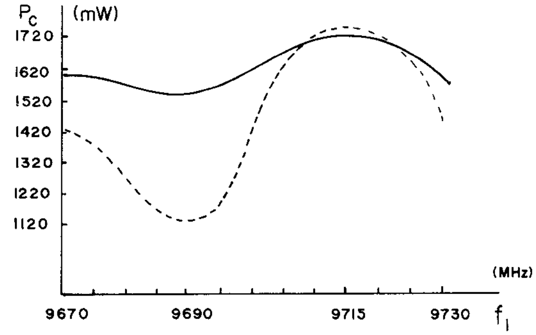

Fig. 4. Tuning characteristics of the 84-oxide combiner. Solid curve: experimental results. Broken curve: calculated results.

over the synchronization range. Adjusting ω_1, ω_2, and ω_3 to set $\delta_2 = \delta_{2\,op}$ and $\delta_3 = \delta_{3\,op}$ will maximize the output power

$$\begin{aligned} P_c &= |a_2|^2_{max} + |a_3|^2_{max} \\ &= \alpha^2 P_1 + P_2 + \beta^2 P_1 + P_3 \\ &= P_1 + P_2 + P_3 \end{aligned} \tag{8}$$

provided that

$$Q_{ex2}\delta_{2\,op} = Q_{ex3}\delta_{3\,op} \tag{9a}$$

$$\alpha^2 P_2 - \beta^2 P_3 = (\beta^2 - \alpha^2)P_1. \tag{9b}$$

This indicates that the sum of the maximum power is delivered to the load.

In practice the number of couplers with different coupling coefficients is limited and the oscillators to be combined may exhibit characteristics far from the requirements of (9). Because of this, losses will arise in the combiner circuit. These losses appear as power reflected back to oscillator 1, i.e., $b_1 \neq 0$. Under such conditions the output power is given by

$$P_c = P_1 + P_2 + P_3 - |b_1|^2 \tag{10}$$

and defining a combining efficiency as $\eta_c = (P_c/(P_1 + P_2 + P_3))\cdot 100$ percent one obtains

$$\eta_c = \frac{\beta^2(\alpha^2 P_1 + P_2) + \alpha^2(\beta^2 P_1 + P_3) + 2\alpha\beta\sqrt{(\alpha^2 P_1 + P_2)(\beta^2 P_1 + P_3)}}{P_1 + P_2 + P_3} \cdot 100 \text{ percent.} \tag{11}$$

Fig. 5 represents the influence of the characteristics of the oscillators on the circuit operation of the combiner for a 3-dB coupler. The abscissa plots the deviations of the power levels P_2 and P_3 from the values satisfying (9) while the ordinate is referenced to the calculated combining efficiency. For $P_2 = P_3$, combining efficiency takes its peak (100 percent) and remains higher than 90 percent so long as the difference between P_2 and P_3 is less than 6 dB. This promises a good circuit tolerance to dissimilar oscillators.

B. Output Frequency and Injection Locking of the Combiner

Under the conditions of (9) the synchronization frequency, i.e., the output frequency ω_c of the combiner, is equal to ω_1 which is necessarily higher than ω_2 and ω_3 from Fig. 2. But when the conditions do not hold, $b_1 \neq 0$ and a

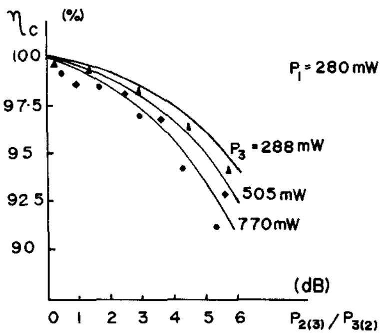

Fig. 5. Effect of the difference between P_2 and P_3 on the combining efficiency for a 3-dB short slot coupler $\alpha=\beta=1/\sqrt{2}$. Experimental results—rectangles: 84-diode combiner; triangles: 60-diode combiner; circles: 36-diode combiner.

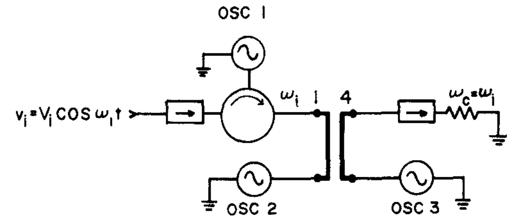

Fig. 6. Arrangement for injection-locking of the combiner.

signal with frequency lower than ω_1 synchronizes oscillator 1. Subsequently the system becomes mutually synchronized and ω_c is no longer equal to ω_1. It will be slightly lower than it and higher than ω_2 and ω_3.

To control ω_c, the injection-locking arrangement of Fig. 6 can be employed. Using an isolator and circulator, oscillator 1 is injection-locked to the external signal $v_i = V_i \cos \omega_i t$. The frequency of the signal going into port 1 of the coupler is determined by ω_i. Since any signal reflected back to this port is absorbed by the isolator, no mutual synchronism occurs and the combiner will be injection-locked to the external signal giving $\omega_c = \omega_i$.

III. Experimental Results

The operation of the combiner circuit just described, has already been experimentally confirmed using single-diode oscillators [6]. The experiments carried out here apply the circuit to combine multiple-diode oscillators to extend the total number of devices combined.

A. Multiple-Device Oscillators

The multiple-device oscillators used in the experiments should meet the two following requirements: 1) the oscillators must be stable during circuit adjustment; 2) the oscillators' circuit design must be applicable to a relatively large number of devices (this permits one to increase the total number of devices at will).

We selected the Kurokawa oscillator [1]. One 12-diode and two 36-diode oscillators were constructed using X-band Gunn diodes (NEC GD-511AA, 15–30 mW). The output power as well as the external Q of each oscillator operating at 9.7 GHz is presented in Table I. The best position to tune the frequency of the oscillators was found to be at the point of maximum electric field located a quarter-guide wavelength from the front of the oscillator cavity. Using a capacitive screw, each oscillator could be tuned over 120 MHz with 0.13-dB power variation.

TABLE I
The Output Power and Q_{ex} of Multiple-Diode Oscillators

OSC. NO.	POWER (mW)	Q_{ex}
12-DIODE OSC.	280	438
36-DIODE OSC. NO.1	700	177
36-DIODE OSC. NO.2	770	194

TABLE II
Results of 84-Diode Power Combining

	FREE RUNNING						COMBINED		
	FREQ. DEVIATION (MHz)			POWER (mW)			FREQ. (MHz)	POWER (mW)	EFF. (%)
	Δf_1	Δf_2	Δf_3	P_1	P_2	P_3	f_c	P_c	η_c
MEAS.	5	-30	-20	280	700	770	9710	1720	98.3
CALCU.		-20	-15					1732	99.3

B. 84-Diode Power Combiner

By connecting the 12-diode oscillator to port 1 and the 36-diode oscillators to ports 2 and 3 of a 3-dB short slot coupler, we have built an 84-diode power combiner.

First, to obtain the maximum output power P_c, the oscillation frequencies of the oscillators were adjusted. The results are summarized in Table II. The oscillation frequencies and output powers of individual oscillators are given in $\Delta f_j = f_j - f_c$, and P_j, respectively, where $j = 1,2,3$ and f_c is the output frequency. The combining efficiency η_c and output power P_c are also presented. The results of theoretical calculations to obtain the maximum P_c are also given in Table II. To derive those values use is made of Table I, (2), (3), (10), (11), and the value of f_1 from the experiment. The differences between the experimental and theoretical results represent the fact that a signal reflected into port 1 has synchronized oscillator 1.

Next, to examine the tuning characteristics of the combiner, the circuit was first adjusted for maximum output power and then oscillator 1 was tuned alone over the synchronization range. The effect of such tuning on the output power is shown by solid curve in Fig. 4. The combiner remained frequency synchronized over 60 MHz with 0.57-dB change in power level. The broken curve in Fig. 4 plots $\hat{P}_c$ from (7) using the given parameters of the oscillators. The deviation between the curves reflects the fact that to derive P_c no effect of reverse injection into oscillator 1 is taken into account. However, this happy occurence, at frequencies far from the optimum, improves the overall behavior of the combiner.

Finally, the injection-locking behavior of the combiner was tested using the setup of Fig. 6. After adjusting the circuit for maximum output power, the injection signal was applied and the output power and output frequency were monitored while sweeping the injection frequency. The results are shown in Fig. 7 with the injection power P_i as a parameter. As the injection power level increases the locking bandwidth becomes wider. For very large injection

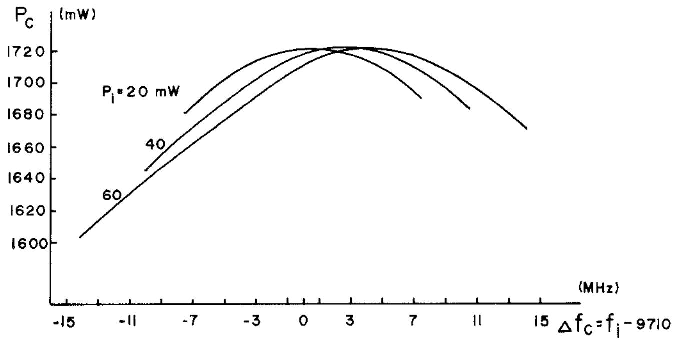

Fig. 7. Injection-locking behavior of the 84-diode combiner.

TABLE III
RESULTS OF 60- AND 36-DIODE POWER COMBINING

		FREE RUNNING						COMBINED		
		FREQ. DEVIATION (MHz)			POWER (mW)			FREQ. (MHz)	POWER (mW)	EFF. (%)
		Δf_1	Δf_2	Δf_3	P_1	P_2	P_3	f_c	P_c	η_c
60-DIODE COMB.	MEAS.	4	-23	-20	280	400	505	9688	1160	97.8
	CALCU.		-15	-18					1170	99
36-DIODE COMB.	MEAS.	3	-19	-17	280	283	288	9685	850	99.8
	CALCU.		-11	-11					860	99.9

power level, as the injection frequency is swept over the locking range, the change in the output power from its peak becomes rapid however. So, a compromising effort can be made between the injection-locking stability of the system and the changes in the output power level.

C. 60- and 36-Diode Power Combiners

To investigate the effect of the number of devices combined on the circuit operation we have also constructed 60- and 36-diode combiners. Oscillators 2 and 3 of the previous combiner were replaced by two 24-diode oscillators ($Q_{ex2} = 290$, $Q_{ex3} = 242$) to construct a 60-diode combiner, and by two 12-diode oscillators ($Q_{ex2} = Q_{ex3} = 438$) to build a 36-diode combiner, respectively. The results of circuit adjustments for maximum output power from the experiments and calculations are summarized in Table III.

With regard to Tables II and III, as the total number of devices contributed by oscillators 2 and 3 increases the degree of detuning δ increases. The reason can be explained as follows. By increasing the number of devices per oscillator their external Q's are reduced [11]. Therefore, for a given $Q_{ex}\delta_{op}$, δ_{op} should be increased to compensate for the reduction of Q_{ex} in order to operate each synchronized oscillator under its maximum output power condition (Fig. 2).

From all the combiners built, combining efficiencies of about 100 percent, not higher, at stable operation, were obtained. The main reason for the slight deviation from 100 percent is that the parameters of oscillators 2 and 3 do not satisfy (9). The deviation is, for example, less than 2 percent for a 105-mW difference between power levels P_2 and P_3 for 60-diode combiner. This exhibits a good circuit tolerance of the combiner with respect to the dissimilarity of oscillators to be used (Fig. 5).

IV. CONCLUSIONS

By incorporating two groups of combiners a method was developed to increase the total number of devices that can be combined. The combiner circuit consisting of 3 oscillators and a directional coupler was analyzed by employing oscillator synchronization theory. Conditions for optimum operation of the combiner were established. A prototype 84-diode power combiner was constructed and the total output power of 1.72 W with combining efficiency of 98.3 percent at 9.7 GHz was obtained. The injection-locking experiment with the prototype combiner resulted in 28 MHz of locking bandwidth at a gain of 16.3 dB. We have also built power combiners including 60 and 36 diodes to demonstrate output power of 1.16 and 0.85 W with combining efficiencies of 97.8 and 99.8 percent, respectively, at 9.6 GHz. It was found that the performance of the circuit is not seriously affected by the dissimilarity of the oscillators used; combining efficiency remains higher than 90 percent so long as the difference between the power level of the oscillators is less than 6 dB. No fundamental limiting factor for the maximum number of devices that can be combined was found. The experiments described, have been conducted at X-band using low power Gunn diodes. The combining scheme can be, however, applied to higher frequency bands and other high power devices such as IMPATT's.

REFERENCES

[1] K. Kurokawa, "The single-cavity multiple-device oscillator," *IEEE Trans. Microwave Theory Tech.*, vol. MTT-19, pp. 793–801, Oct. 1971.

[2] R. S. Harp and H. L. Stover, "Power combining of X-band IMPATT circuit modules," presented at the 1973 IEEE Int. Solid-State Circuit Conf., Feb. 1973.

[3] S. E. Hamilton, "32-diode waveguide power combiner," presented at the 1980 IEEE Microwave Theory Tech. Symp., May 1980.

[4] M. Nakajima, "A proposed multistage microwave power combiner," *Proc. IEEE*, vol. 61, pp. 242–243, Feb. 1973.

[5] J. R. Nevarez and G. J. Herskowitz, "Output power and loss analysis of 2^n injection-locked oscillators combined through an ideal and symmetric hybrid combiner," *IEEE Trans. Microwave Theory Tech.*, vol. MTT-17, pp. 2–10, Jan. 1969

[6] S. Mizushina, H. Kondoh, and M Ashiki, "Corporate and tandem structures for combining power from 3^N and $2N+1$ oscillators," *IEEE Trans. Microwave Theory Tech.*, vol. MTT-28, pp. 1428–1432, Dec. 1980.

[7] J. L. Altman, *Microwave Circuits.* New York: Van Nostrand, 1964, ch. 3, pp. 115–125.

[8] Y. Tanimoto, M Makajima, and J. Ikenoue, "A traveling-wave approach to injection-locking of microwave oscillators" (in Japanese), presented at the Osaka-Kyoto Regional Meeting of Radiation Science Group, Dec. 1976.

[9] M. Nakajima and J. Ikenoue, "Locking phenomena in microwave oscillator circuits," *Int. J. Electron.*, vol. 44, pp. 465–472, May 1978.

[10] K. Kurokawa, "Injection-locking of microwave solid-state oscillators," *Proc. IEEE*, vol. 61, pp. 1386–1410, Oct. 1973.

[11] R Aston, "Techniques for increasing the bandwidth of a TM_{010}-mode power combiner," *IEEE Trans. Microwave Theory Tech.*, vol. MTT-27, pp. 479–482, May 1979.

Mohammad Madihian (S'78) was born in Tehran, Iran, on January 3, 1954. He received the B.Sc. degree from the Iran College of Science and Technology, Tehran, Iran, in 1976, and the M.Sc. degree from Shiz-

uoka University, Hamamatsu, Japan, in 1980, both in electronic engineering.

He is currently studying towards the Ph.D. degree in electronics at the Research Institute of Electronics, Shizuoka University, Hamamatsu, Japan, where he is primarily involved in microwave solid-state oscillators design and power combining schemes.

Mr. Madihian is a member of the Institute of Electronics and Communication Engineers of Japan.

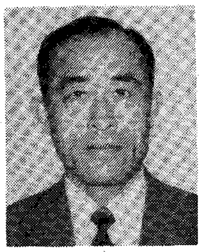

Shizuo Mizushina (S'60–M'66) was born in Hamamatsu, Japan, on August 10, 1933. He received the B. Eng. degree from Shizuoka University, Hamamatsu, in 1957, and the M.Sc. and Ph.D. degrees from Ohio State University, Columbus, in 1962 and 1964, respectively.

From 1957 to 1960 he was a Research Assistant and Lecturer at Shizuoka University. From 1964 to 1965 he was a Member of the Technical Staff at the Bell Telephone Laboratories, Murray Hill, NJ. In 1965 he returned to Shizuoka University where he is a Professor at the Research Institute of Electronics. He has worked on millimeter-wave magnetrons, gigabit-pulse regenerators, solid-state oscillators, and device-circuit interaction problems. His current research interests are concerned with microwave power-combining techniques, microwave thermography, and medical electronics.

Dr. Mizushina is a member of the Institute of Electronics and Communication Engineers of Japan, the Japan Society of Medical Electronics and Biological Engineering, and Sigma Xi.

Simulation Study of Harmonic Oscillators

KLAUS SOLBACH, MEMBER, IEEE

Abstract —**In the last few years, the operating modes of Gunn oscillators for frequencies above 60 GHz have been discussed controversially. In this context, a general theoretical circuit model for oscillators operating in the fundamental and in the second-harmonic modes is studied. The model employs a simple cubic $I-V$ characteristic of the active element and separate embedding circuits for the fundamental and second-harmonic frequencies. The current and voltage waveforms of both modes are contrasted. The oscillator source impedances and the external Q of the second-harmonic mode oscillator are calculated.**

I. Introduction

During the last years, several papers have been published concerning the design of second-harmonic GaAs Gunn oscillators for frequencies between 50 and 110 GHz, as well as concerning methods for the classification of existing oscillator designs in terms of the harmonic number [1]–[4]. Indeed, there has been wide unawareness of the possibility of harmonic operation of Gunn oscillators in the past. Such oscillator design as the cap-structure oscillator, used, e.g., by Ondria [5] for GaAs Gunn devices up to frequencies of 110 GHz, exhibited uncommonly high external quality factors Q_e and it was observed that a backshort would have practically very little influence on the oscillator frequency. Attempts were made in the past to explain this unusual behavior by proposing that the Gunn elements were operated in other modes, like the quenched space-charge mode or a hybrid mode.

Manuscript received February 4, 1982; revised April 14, 1982.
The author is with AEG-Telefunken, A1E32, D-7900 Ulm, West Germany.

Barth was one of the first researchers to propose that this behavior would best be explained by assuming the oscillators to be operated as harmonic generation circuits, and he demonstrated this approach to be very efficient in the design of a wide-band-tunable W-band Gunn oscillator [1].

Two experiments have been reported [3], [4], which analyze the harmonic behavior of GaAs Gunn oscillators of the cap type. It is now clear that efficient second-harmonic generation is feasible in the frequency range up to 110 GHz using GaAs Gunn elements and it is reasonable to suspect earlier published oscillator work relied on the same principle.

In this paper, an effort is made to contrast the fundamental circuit behavior of a negative resistance element operated in the fundamental mode with that operated in the second-harmonic mode. A simple nonlinear negative resistance description for the active element is adopted. This $I-V$ characteristic is not a static property of the active element (needs not be valid for dc), but it basically describes that the element at a certain frequency has the ability to generate oscillations (negative resistance) which are limited in amplitude (nonlinearity). Although this description of the element properties is rather general, it has been shown that the fundamental circuit behavior of the fundamental-mode operation of Gunn oscillators may be modeled very well [7]. For Tunnel diodes and one-port-transistor circuits, the model is even more realistic since these elements exhibit static and/or dc current–voltage characteristics very similar to the form employed here.

0018-9480/82/0800-1233$00.75